Published OnlineFirst August 18, 2009; DOI: 10.1158/0008-5472.CAN-09-1684

Identification of a Stat3-Dependent Transcription Regulatory Network Involved in Metastatic Progression

Jill J. Ranger,[1,3] David E. Levy,[6] Solmaz Shahalizadeh,[1,2,5] Michael Hallett,[1,2,3,5] and William J. Muller[1,3,4]

[1]Goodman Cancer Centre, [2]Centre for Bioinformatics, Departments of [3]Biochemistry and [4]Medicine, and [5]School of Computer Science, McGill University, Montreal, Quebec, Canada and [6]Departments of Pathology (Experimental) and Microbiology, New York University School of Medicine, New York, New York

Abstract

High levels of activated Stat3 are often found in human breast cancers and can correlate with poor patient outcome. We employed an activated ErbB2 mouse model of breast cancer to investigate the *in vivo* role of Stat3 in mammary tumor progression and found that Stat3 does not alter mammary tumor initiation but dramatically affects metastatic progression. Four-fold fewer animals exhibited lung metastases in the absence of Stat3 and a 12-fold reduction in the number of lung lesions was observed in animals bearing Stat3-null tumors when compared with the wild-type cohort. The decreased malignancy in Stat3-deficient tumors is attributed to a reduction in both angiogenic and inflammatory responses associated with a Stat3-dependent transcriptional cascade involving CCAAT/enhancer binding protein δ. [Cancer Res 2009;69(17):6823–30]

Introduction

Constitutive activation of the transcription factor Stat3 is observed in 35% to 60% of human breast cancers (1, 2) and in a wide variety of other cancer types (3). In normal tissues, Stat3 is involved in the direct transcriptional regulation of targets downstream of both cytokine and growth factor receptors. In tumors, Stat3 is activated downstream of oncogenes such as ErbB2/Neu, PyVMT, and Src (4–6). Overexpression of constitutively activated forms of Stat3 in fibroblast cells, either in isolation or in conjunction with oncogenes, induces the formation of foci *in vitro* and tumors in orthotopic mouse models (6, 7). Moreover, loss of Stat3 function via RNA knockdown (8, 9), peptide inhibition (10), and expression of dominant-negative forms (6, 11, 12) in cancer cells leads to a decrease in tumor cell growth and angiogenesis with a concomitant increase in apoptosis (9, 12, 13). Analyses of human tumor tissues have also shown that Stat3 expression and activation correlates with tumor grade, stage, or the presence of metastases (1, 14–16).

Whereas studies suggest that activation of Stat3 is a critical event in the transformation of established cell lines *in vitro*, the *in vivo* role of Stat3 in mammary tumorigenesis is still unknown. To investigate the role of Stat3 in breast cancer, conditional Stat3 (Stat3flx) mice (17) were interbred with a novel transgenic strain (MMTV-NIC) where the expression of an activated form of ErbB2 is coupled to Cre recombinase via an internal ribosome entry site (18). The resulting $Stat3^{flx/flx}$/NIC mice exhibited an ~4-fold reduction in the incidence of tumor metastasis relative to the parental NIC strain, although tumor onset was not altered by mammary-specific, Cre-mediated ablation of Stat3. Using gene expression profiling, we observed that *cebpd* was down-regulated in the Stat3-deficient tumors relative to their wild-type counterparts. Consequently, $Stat3^{flx/flx}$/NIC tumors lacked the ability to induce the expression of acute-phase response (APR) genes downstream of both Stat3 and CCAAT/enhancer binding protein (C/EBPδ; ref. 19). These results suggest that Stat3 may mediate a tumor inflammatory response through several downstream APR genes and thus provide a prometastatic tumor environment.

Materials and Methods

Transgenic mice. Mice harboring the conditional *stat3* allele were generated in the Levy laboratory and characterized previously (17, 20). MMTV-NIC transgenic mice were generated as described (18). All mice were housed in the animal facility of the Royal Victoria Hospital and all experiments were done in accordance with the animal care guidelines at the Animal Resource Centre of McGill. Mammary tumors were detected via biweekly physical palpation and animals were sacrificed 6 weeks following initial palpation. Material from necropsied mice was frozen in liquid nitrogen (in some cases, tissues were set in an OCT medium before freezing) or was fixed in 10% neutral buffered formalin and embedded in paraffin wax. Fixed and embedded mammary tumors and lung lobes were sectioned at 4 μm and either stained by H&E or processed further as indicated. Five H&E-stained lung sections, taken at 50 μm intervals, were examined by microscope for metastatic lesions. Experimental metastasis assays were performed by injecting 5×10^5 cells into the lateral tail vein of NCr mice (Taconic). Lungs were collected and processed as described above at 4 weeks post-injection.

Primary cell culture. $Stat3^{wt/wt}$/NIC or $Stat3^{flx/flx}$/NIC mammary tumors were excised, finely chopped, and dissociated in DMEM (Wisent) containing 2.4 mg/mL collagenase B (Roche) and 2.4 mg/mL Dispase II (Roche) for 3 h at 37°C, with constant agitation. The cell suspensions were centrifuged at 1,000 rpm for 5 min, washed in a PBS/EDTA solution, and respun at 1,000 rpm for 5 min. Pellets were resuspended in DMEM containing 10% fetal bovine serum (Wisent), MEGM SingleQuots (Clonetics), and 5% penicillin/streptomycin (Wisent). Cells were counted and plated on 10 cm Nunc dishes.

Immunoblotting, ELISA, and immunohistochemical analyses. Frozen mammary tumors were lysed using a PLC-γ buffer and run on SDS-PAGE gels. Proteins were detected with antibodies against Stat3, Stat3-Y705-P (1:1,000; 9132 and 9131; Cell Signaling), Neu (1:1,000; sc284; Santa Cruz Biotechnology), vascular endothelial growth factor (VEGF; 1:1,000, PC315; Calbiochem), β-actin (1:1,000; A5441; Sigma), and Grb2 (1:1,000; sc255; Santa Cruz Biotechnology). Tumor lysate VEGF was measured with a mouse Quantikine ELISA kit (MMV00; R&D Systems). Immunohistochemical analyses were performed on paraffin or OCT-embedded sections as

Note: Supplementary data for this article are available at Cancer Research Online (http://cancerres.aacrjournals.org/).

Requests for reprints: William J. Muller, McGill University, Cancer Pavilion, Room 509, 1160 Pine Avenue West, Montreal, Quebec, Canada H3G 0B1. Phone: 514-398-5847; Fax: 514-398-6769; E-mail: William.muller@mcgill.ca.

doi:10.1158/0008-5472.CAN-09-1684

Published OnlineFirst August 18, 2009; DOI: 10.1158/0008-5472.CAN-09-1684

described previously (18). Antibodies used for immunohistochemical analyses include Stat3 (1:100; 9139; Cell Signaling), Stat3-Y705-P (1:50; 9145; Cell Signaling), and Cre (1:600; PRB106C; Covance). Staining for CD31 (1:100; 550274; BD Biosciences), Ki-67 (1:1,000; ab15580; Abcam), and terminal deoxynucleotidyl transferase–mediated dUTP nick end labeling (Apoptag Peroxidase Detection kit; Chemicon) was quantified using slides scanned with a Scanscope XT Digital Slide Scanner (Aperio) and corresponding positive pixel and nuclear immunohistochemical algorithms.

Microarray experiments. Total RNA was extracted from flash-frozen mammary tumor samples using a Qiagen RNeasy Midi kit and labeled using an Amino Allyl MessageAmp II aRNA Amplification Kit (Applied Biosystems) and Cy3 and Cy5 dyes (Amersham Biosciences) in preparation for microarray hybridization. Dye-labeled RNA was hybridized onto a Whole Mouse Genome Oligo 4 × 44 K Microarray platform (Agilent) against a universal mouse reference RNA (Stratagene). The resulting arrays were scanned using a Microarray Scanner (model G2565BA; Agilent Technologies) and processed using Feature Extraction software (Agilent). Data processing, normalization, and analysis were carried out using BIAS system (21). RMA background correction algorithm was used for correcting raw feature intensities (22). Resulting expression estimates were converted to $\log_2$ ratios. Spatial and intensity-dependent Loess was done to normalize within arrays (23). Median absolute deviation scale normalization was used to normalize between arrays (24). Differentially expressed genes were detected using rank product nonparametric statistic (P = 0.01; ref. 25). Microarray results have been deposited in the Gene Expression Omnibus database under the accession number GSE15632.

Results

Stat3 is not required for the initiation of mammary tumors but is important for tumor cell proliferation. To study Stat3 loss in a mouse model of tumorigenesis, we used Stat3 conditional mice harboring either one or two loxP-flanked *stat3* alleles (*stat3flx*; ref. 17). To circumvent the stochastic expression of Cre observed in many MMTV-Cre–based models (26), we mated the *stat3flx* animals with the transgenic NIC strain (18). In this model, mammary epithelial cells that express the activated ErbB2 oncogene will simultaneously express Cre recombinase resulting in the deletion of the conditional *stat3* allele (18).

To investigate the role of Stat3 in the induction of mammary tumors, cohorts of virgin female Stat3$^{wt/wt}$/NIC, Stat3$^{flx/wt}$/NIC, and Stat3$^{flx/flx}$/NIC mice were generated. All cohorts developed mammary tumors with statistically similar average onsets of 4.7 ± 0.1, 4.4 ± 0.1, and 4.6 ± 0.1 months, respectively (Fig. 1*A*). We verified the Cre recombinase-mediated *stat3* deletion in the tumors from all three cohorts using PCR analyses (Supplementary Fig. S1). Ablation of Stat3 at the protein level was confirmed by both immunoblot and immunohistochemical analyses (Fig. 1*B* and *C*). Despite the fact that levels of Stat3 and its activated form, phospho-Y705-Stat3, were significantly reduced in Stat3$^{flx/flx}$/NIC tumors (Fig. 1*B* and *C*), total activated ErbB2 protein did not change across the samples (Fig. 1*B*). Tumors from NIC animals heterozygous for the *stat3flx* allele expressed total and activated Stat3 protein at levels comparable with the wild-type NIC tumors (data not shown). The residual Stat3 protein observed in Stat3$^{flx/flx}$/NIC mammary tumor lysates (Fig. 1*B*) is due to the retention of an intact *stat3flx* allele in the stroma as evidenced by a faint band by PCR (Supplementary Fig. S1) and by Stat3-positive stromal cells detected in the Stat3$^{flx/flx}$/NIC tumor sections (Fig. 1*C*). Histologic analysis of H&E-stained tumor sections showed that the Stat3$^{flx/flx}$/NIC tumors displayed characteristics of solid adenocarcinomas similar to wild-type activated ErbB2-driven tumors (Fig. 1*C*). Thus,

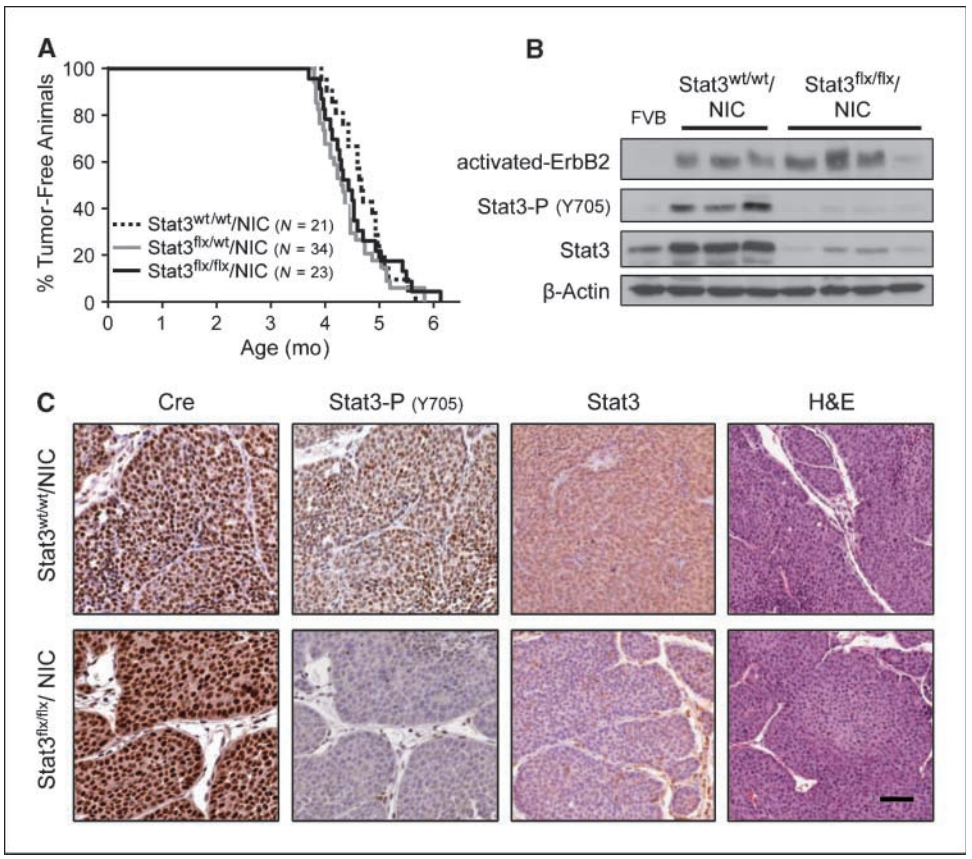

Figure 1. Stat3 activation is not required for the initiation of mammary tumorigenesis. *A,* mammary tumor onset in Stat3$^{wt/wt}$/NIC, Stat3$^{flx/wt}$/NIC, and Stat3$^{flx/flx}$/NIC cohorts (T_{50} = 4.7, 4.3, and 4.5 mo, respectively). *B,* immunoblot analysis of Stat3 and activated ErbB2 expression in mammary tumor cell lysates from Stat3$^{wt/wt}$/NIC and Stat3$^{flx/flx}$/NIC animals. *C,* staining of paraffin-embedded sections of mammary tumors using antibodies against Cre (*leftmost column*), Stat3-Y705P and Stat3 (*middle columns*), or H&E (*rightmost column*). *Bar,* 50 μm.

Published OnlineFirst August 18, 2009; DOI: 10.1158/0008-5472.CAN-09-1684

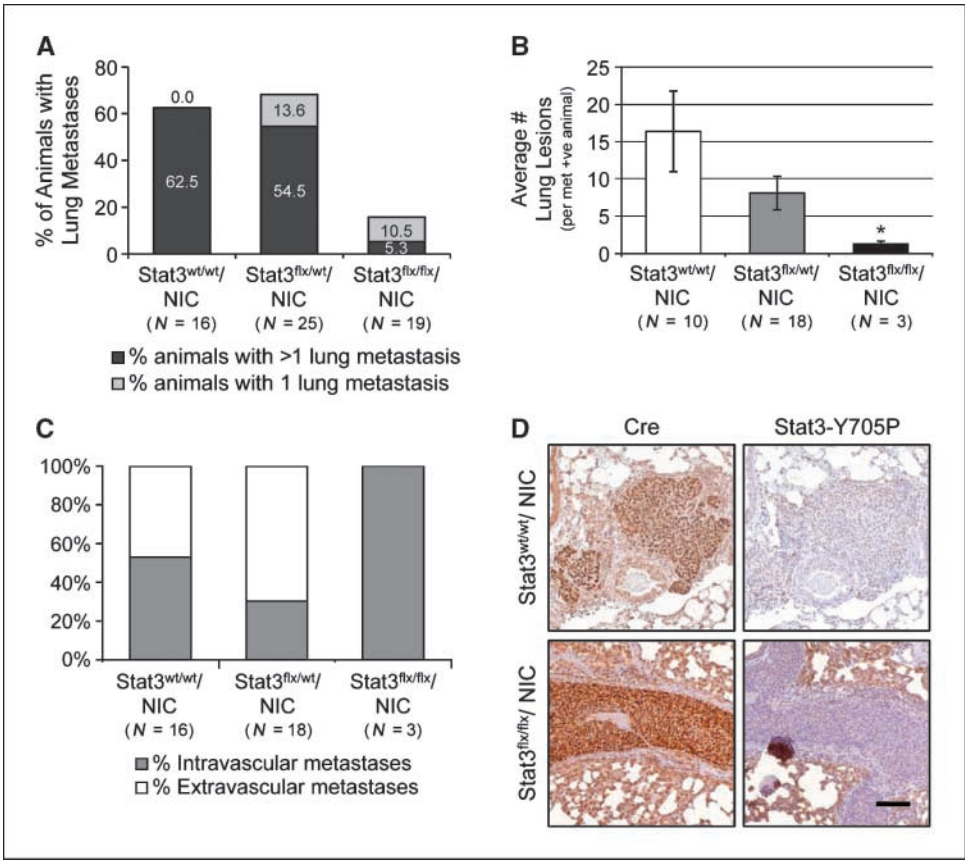

Figure 2. The presence of lung metastases is greatly reduced in mice bearing $Stat3^{flx/flx}$/NIC mammary tumors. Percentage of $Stat3^{wt/wt}$/NIC, $Stat3^{flx/wt}$/NIC, and $Stat3^{flx/flx}$/NIC animals harboring metastatic lesions in the lung (*A*) and quantification of the average ± SE number of lesions per lung from animals positive for lung metastases (*B*). *C,* percentage of intravascular versus extravascular lung lesions. *D,* immunohistochemical anti-Cre (*right*) and anti-Stat3Y705P (*left*) staining of paraffin-embedded lung sections from $Stat3^{wt/wt}$/NIC and $Stat3^{flx/flx}$/NIC animals. *Bar,* 100 μm. *, $P = 0.021$, two-tailed Student's *t* test.

$Stat3^{flx/flx}$/NIC mice develop Stat3-null mammary epithelial tumors with the same onset as the wild-type NIC group.

Although mammary epithelial disruption of Stat3 had no affect on the initiation of NIC tumors, Stat3 activation has been reported to enhance tumor growth in some *in vitro* studies (12, 27). Therefore, the total tumor burden in $Stat3^{wt/wt}$/NIC, $Stat3^{flx/wt}$/NIC, and $Stat3^{flx/flx}$/NIC mice was measured at sacrifice (6 weeks post-palpation). Wild-type NIC animals exhibited an average total tumor volume of 3.5 ± 0.4 cm^3, whereas the total volume measured in $Stat3^{flx/wt}$/NIC and $Stat3^{flx/flx}$/NIC was 1.7 ± 0.2 and 2.1 ± 0.4 cm^3, respectively (Supplementary Fig. S2*A*). Impaired tumor growth was attributed to >2-fold reduction in the number of proliferating cells in the Stat3-deficient mammary tumors as assessed by Ki-67 immunohistochemical staining (Supplementary Fig. S2*B*) and not to a change in the apoptotic status of the same cells as determined by a terminal deoxynucleotidyl transferase–mediated dUTP nick end labeling assay (Supplementary Fig. S2*C*). We also counted the number of tumors present in end-stage animals. Multifocal tumors were observed in nearly all the tumor-bearing $Stat3^{wt/wt}$/NIC and $Stat3^{flx/wt}$/NIC mice: >92.5% in both cases (Supplementary Fig. S3*A*). In contrast, only 62.5% of the $Stat3^{flx/flx}$/NIC tumor-bearing animals developed multifocal tumors (Supplementary Fig. S3*A*). In addition, analysis of the adjacent tumor-free inguinal mammary glands from tumor-bearing mice at end-stage revealed that animals lacking Stat3 in the mammary epithelium developed ~12 times fewer lesions than either wild-type or heterozygous animals (Supplementary Fig. S3*B* and *C*). Taken together, these observations suggest that whereas Stat3 is dispensable for the initiation of activated ErbB2-induced mammary tumors, its loss causes a statistically significant reduction in total tumor burden attributed to both reduced tumor proliferation and penetrance.

Stat3 plays a critical role in the metastasis of ErbB2-driven mammary tumors. We next examined whether loss of Stat3 altered the metastatic capacity of ErbB2-induced tumors. Lungs from $Stat3^{wt/wt}$/NIC, $Stat3^{flx/wt}$/NIC, and $Stat3^{flx/flx}$/NIC tumor-bearing mice were taken at 6 weeks post-palpation and scored for the presence of metastatic lesions. Only 15.8% of $Stat3^{flx/flx}$/NIC animals exhibited lung lesions compared with 62.5% incidence in the wild-type NIC cohort (Fig. 2*A*). Notably, mice heterozygous for the conditional *stat3* allele, which presented with a statistically similar ($P = 0.47$) tumor burden to the $Stat3^{flx/flx}$/NIC mice (Supplementary Fig. S2*A*), exhibited comparable rates of metastasis to the wild-type NIC animals (Fig. 2*A*). This precludes the possibility that the reduced tumor volume in the $Stat3^{flx/flx}$/NIC cohort is responsible for the ~4-fold reduction in metastasis seen in the homozygous group (Fig. 2*A*). These results show that Stat3 is nearly indispensable for metastasis of activated ErbB2 tumor cells to the lungs.

We expanded this study to assess the malignancy of the $Stat3^{wt/wt}$/NIC, $Stat3^{flx/wt}$/NIC, and $Stat3^{flx/flx}$/NIC tumors by counting the number of metastases present in the lungs and by characterizing the intravascular or extravascular status of the lesions. The few $Stat3^{flx/flx}$/NIC animals that developed metastases had 12-fold fewer lung lesions on average compared with their wild-type counterparts (Fig. 2*B*). The rare lesions observed in the lungs of $Stat3^{flx/flx}$/NIC mice were strictly confined within the pulmonary vasculature (Fig. 2*C* and *D*), whereas >45% of metastases present in the lungs of $Stat3^{wt/wt}$/NIC and $Stat3^{flx/wt}$/NIC animals

Published OnlineFirst August 18, 2009; DOI: 10.1158/0008-5472.CAN-09-1684

were extravascular, showing the ability of Stat3-proficient tumor cells to invade the surrounding lung parenchyma (Fig. 2*C* and *D*). To verify that the lesions observed in the Stat3$^{flx/flx}$/NIC lungs did not express Stat3, the retention of Cre expression and the loss of active Stat3 in the metastatic lung lesions were confirmed by performing immunohistochemistry with antibodies directed to Cre recombinase and phospho-Y705-Stat3. Lesions from both Stat3$^{wt/wt}$/NIC and Stat3$^{flx/flx}$/NIC lungs revealed high expression of Cre recombinase, whereas only the wild-type–derived metastases retained expression of phospho-Stat3 (Fig. 2*D*). Collectively, these observations argue that Stat3 plays a critical role in the metastatic phase of activated ErbB2 tumor progression.

The metastatic defect in Stat3-deficient tumors correlates with impaired tumor angiogenesis and cell autonomous defects in colonization. To further elucidate the molecular basis for the observed impairment of metastasis in the Stat3-deficient NIC tumors, we assessed whether tumor angiogenesis was affected by ablation of Stat3. Tumor vascularization was quantified by measuring the endothelial content in Stat3$^{wt/wt}$/NIC and Stat3$^{flx/flx}$/NIC tumors stained with an antibody against CD31. Tumors from the Stat3$^{flx/flx}$/NIC animals were less vascularized than tumors from the wild-type cohort (Fig. 3*C*). In addition, a significant reduction of the proangiogenic factor, VEGF (both 50 and 24 kDa isoforms), was observed in the Stat3$^{flx/flx}$/NIC tumors by immunoblotting and ELISA (Fig. 3*A* and *B*). These results indicate that a lack of Stat3 impairs tumor angiogenesis, which may, in turn, impede tumor cell metastasis.

Whereas the above results suggest that defects in the tumor microenvironment may influence the metastatic capacity of Stat3-deficient tumor cells, it is also possible that the inability to efficiently metastasize to the lungs is due to a tumor cell intrinsic defect. To test this possibility, cells from both Stat3-proficient and Stat3-deficient NIC tumors were dissociated and established in cell culture. These primary tumor cells were injected into the lateral tail vein of immunodeficient mice and the number and size of the resulting lung lesions were scored. Injection of Stat3$^{flx/flx}$/NIC tumor cells resulted in a 5-fold reduction in the number and a 12-fold decrease in the size of the resulting lung metastases compared with the Stat3$^{wt/wt}$/NIC tumor cells (Fig. 4*A* and *B*). In addition, the total lung area occupied by metastatic lesions decreased 36-fold in the lungs of animals injected with Stat3$^{flx/flx}$/NIC tumor cells compared with those injected with Stat3$^{wt/wt}$/NIC tumor cells (Fig. 4*C* and *D*). Lesions from these lungs were subjected to immunohistochemical analysis, which recapitulated the results observed in the lesions in the transgenic animals (Supplementary Fig. S4). Before injection, the expression of *erbB2/neu, cre*, and the excision of the *stat3flx* allele was assessed in the Stat3$^{flx/flx}$/NIC tumor cells by PCR on DNA samples from the established mammary epithelial cultures (Supplementary Fig. S5*A*). As with the primary tumors, immunoblotting was performed on protein lysates from the tumor cell cultures (Supplementary Fig. S5*B*). In addition, the proliferative capacity of the primary tumor cells was monitored *in vitro* revealing that, in culture, Stat3-deficient and Stat3-proficient tumor cells grew at the same rate (Supplementary Fig. S5*C*). The fact that these primary Stat3-null tumor cells were impaired in their ability to metastasize even when introduced directly into the vasculature suggests that the metastatic defect observed in the transgenic animals is due only in part to impaired angiogenesis. Indeed, these data suggest that Stat3 also mediates the ability of the tumor cells to colonize and grow in the lung in a cell autonomous manner.

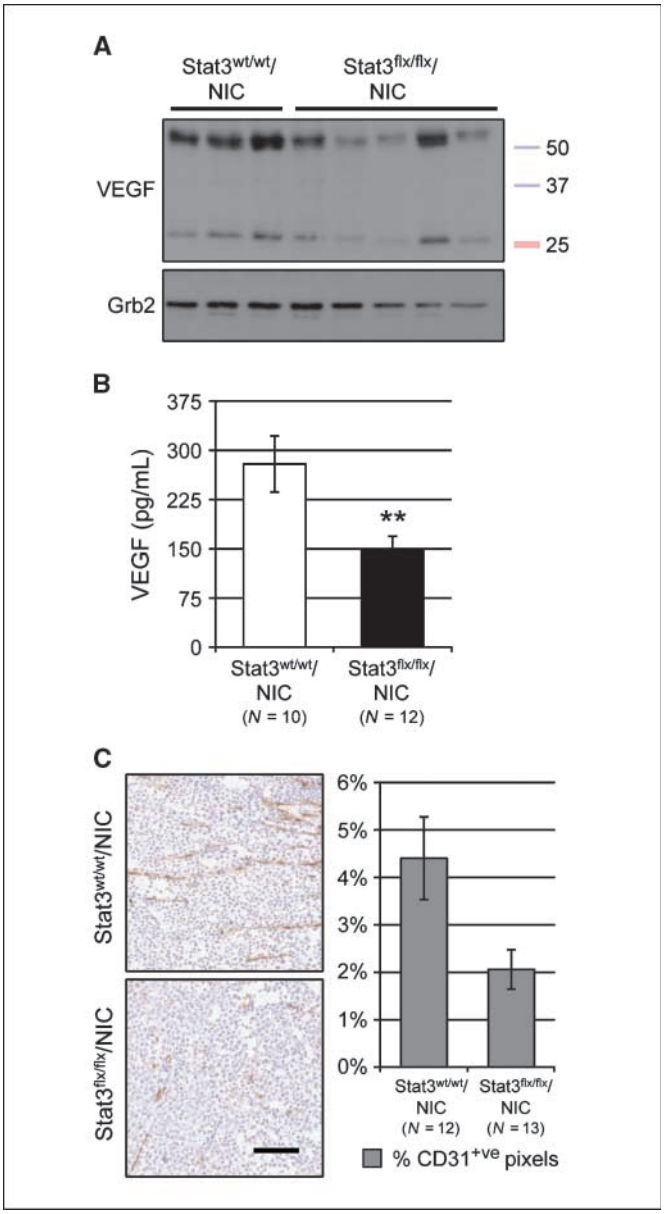

Figure 3. Stat3 ablation leads to decreased VEGF production and angiogenesis. Decreased VEGF protein levels in Stat3$^{flx/flx}$/NIC tumors by immunoblotting (*A*) and ELISA (*B*) assays (average ± SE VEGF quantity). *C,* immunohistochemical staining using a CD31 antibody (*left*) and quantification of the average ± SE number of CD31^{+} pixels (*right*). *Bar,* 100 μm. **, $P = 0.017$, two-tailed Student's *t* test.

Gene expression profiling of Stat3-deficient tumors reveals a Stat3-dependent transcription network involved in the regulation of inflammation and angiogenesis. To further evaluate the impaired metastatic phenotype observed in Stat3$^{flx/flx}$/NIC mice and to identify molecular profiles that would explain the decrease in malignancy, we compared the gene expression profiles of Stat3$^{wt/wt}$/NIC and Stat3$^{flx/flx}$/NIC tumors using Agilent oligonucleotide microarrays. We found that Stat3$^{flx/flx}$/NIC tumors expressed lower levels of both *cebpd* and *osmr*, two genes that are induced by Stat3 (28, 29). These genes code for the transcription factor C/EBPδ and the oncostatin M receptor and are known to potentiate the APR, an early stage of

Published OnlineFirst August 18, 2009; DOI: 10.1158/0008-5472.CAN-09-1684

inflammation. Whereas the oncostatin M receptor acts upstream of Stat3 in the APR, C/EBPδ is a downstream target that promotes the expression of serum amyloid genes, including *saa1* and *saa2* (29, 30). The expression levels of the serum amyloid genes were significantly reduced by >10-fold in the $Stat3^{flx/flx}$/NIC tumors (Fig. 5*A*). We found additional targets involved in the APR and in tumor angiogenesis that were significantly down-regulated in the $Stat3^{flx/flx}$/NIC tumors compared with the wild-type NIC tumors including genes encoding for von Willebrand factor, thrombopoeitin, fibrinogen-γ, fibulin 5, and annexin a3 (Fig. 5*A*). Thus, loss of Stat3 from NIC tumors leads to the down-regulation of many APR and proangiogenic genes, which may lead to reduced tumor inflammation and angiogenesis.

To validate these microarray-based results, we performed quantitative real-time PCR analysis of these candidate genes on total RNA extracted from $Stat3^{wt/wt}$/NIC and $Stat3^{flx/flx}$/NIC tumors. First, we established that *stat3* transcript levels were significantly reduced in the $Stat3^{flx/flx}$/NIC tumors compared with the wild-type tumors (Fig. 5*B*). Next, we determined that the expression levels of direct Stat3 transcriptional targets such as *cebpd* and *osmr* were also reduced by 3.2- and 4.6-fold, respectively. The expression of the direct transcriptional targets of C/EBPδ, *saa1* and *saa2*, was reduced in the $Stat3^{flx/flx}$/NIC tumors by 10.3- and 4.3-fold, respectively (Fig. 5*B*). Given the importance of the Stat3 and C/EBPδ transcriptional network in regulation of the APR and inflammation during normal mammary gland involution (31), these observations suggest that the impaired metastatic phenotype in Stat3-deficient tumors results from a dramatic reduction in tumor inflammation and angiogenesis.

Discussion

The dysregulated activation of Stat3 observed in many human breast cancers (1, 2, 32) suggests that it is of central importance to tumorigenesis and that loss of Stat3 should impair the progression or malignancy of the disease. This is supported by *in vitro* models, where the inhibition of Stat3 alters tumor growth and invasiveness and, in a few cases, prevents tumor initiation (11, 12, 33). Because previous studies were largely based on established tumor cells, the role Stat3 plays in the induction or progression of mammary tumors *in vivo* is still poorly understood. Using a spontaneous transgenic mouse model of tumor progression, we have shown that loss of Stat3 in an activated ErbB2 model of mammary tumorigenesis does not affect the initiation or survival of NIC tumors but does hinder tumor cell proliferation and angiogenesis. The $Stat3^{flx/flx}$/NIC tumors are less metastatic and mammary epithelial cells from these cultures are unable to colonize or grow in the lung. Stat3 ablation also significantly reduced the gene expression of several APR genes including *cebpd, osmr, saa1*, and *saa2*. These results implicate Stat3 in the transcriptional control of tumor inflammation and angiogenesis and suggest a major role for Stat3 expression and activation in the metastatic potential of ErbB2-induced tumors.

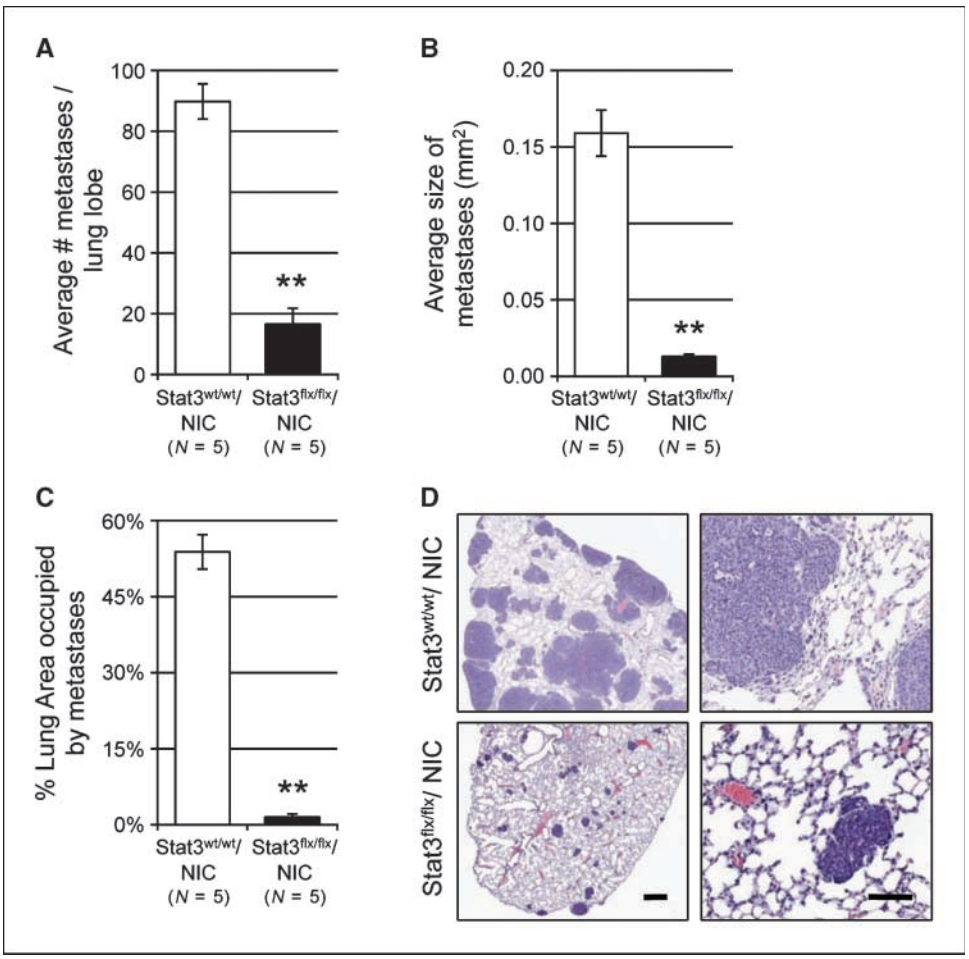

Figure 4. $Stat3^{flx/flx}$/NIC tumor cells show impaired lung colonization in an experimental metastasis assay. Metastatic burden as measured by the average ± SE number of lesions per lung lobe (*A*), average ± SE size of the metastases (*B*), and average ± SE percentage of total lung area covered by metastatic lesions (*C*) based on lesions resulting from experimental metastasis assays using 5×10^5 wild-type or Stat3-null primary tumor cells. *D,* representative H&E-stained sections of lungs from experimental metastasis assays. *Bar,* 0.5 mm (*left column*) and 100 μm (*right column*). *A*, **, *P* = 1.42E-5; *B*, **, *P* = 5.83E-4; *C*, **, *P* = 7.01E-5, two-tailed Student's *t* test.

Published OnlineFirst August 18, 2009; DOI: 10.1158/0008-5472.CAN-09-1684

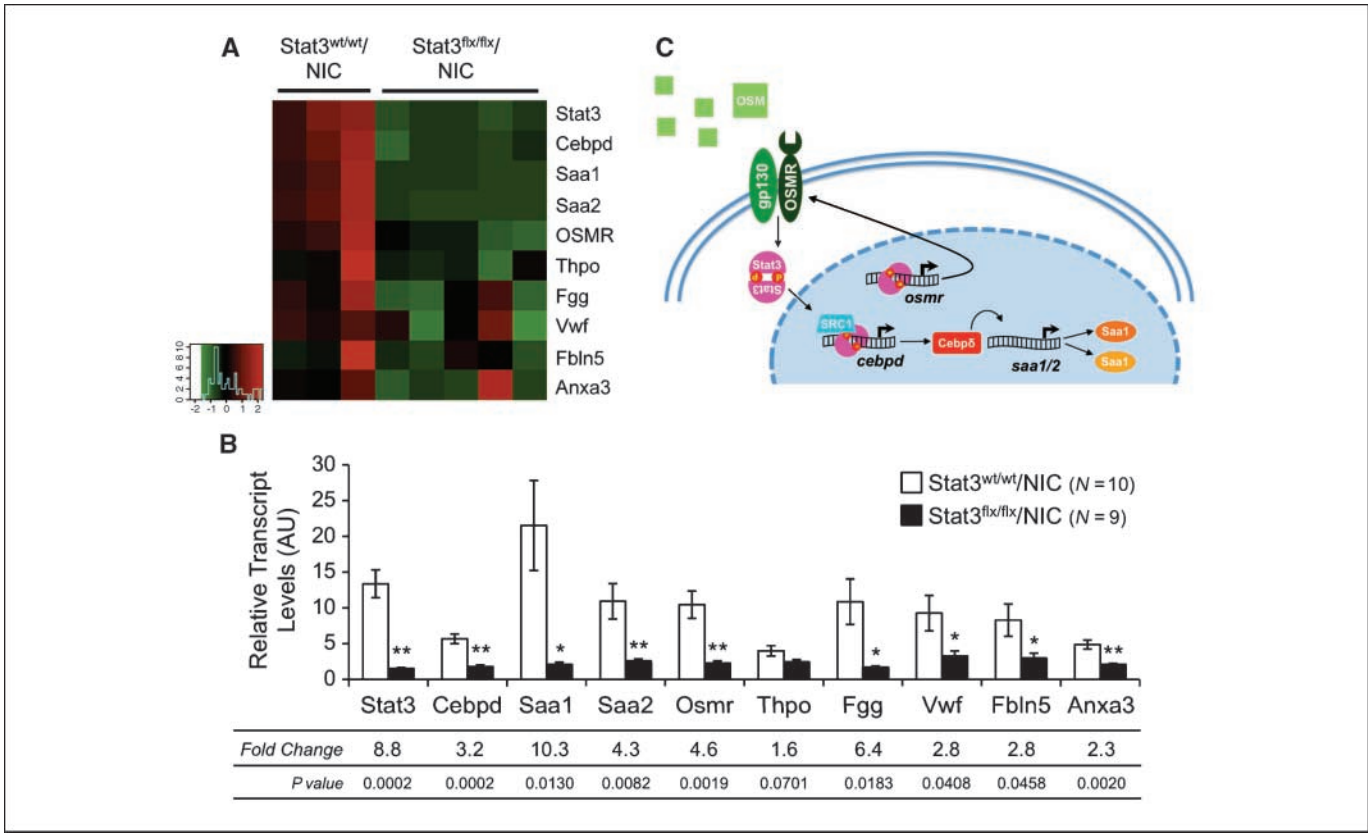

Figure 5. Stat3 expression causes up-regulation of targets involved in angiogenesis and inflammation in NIC tumors. *A,* heat map of selected genes differentially expressed between Stat3$^{wt/wt}$/NIC and Stat3$^{flx/flx}$/NIC tumors. *B,* average ± SE transcript levels of selected genes relative to GAPDH as calculated by quantitative RT-PCR. Fold change calculated by dividing the relative transcript level of the Stat3$^{wt/wt}$/NIC samples by the value for the Stat3$^{flx/flx}$/NIC samples. *C,* schematic of Stat3-dependent transcriptional network controlling inflammation. *P* values were calculated using a Student's *t* test.

Although Stat3 promotes cell death during normal mammary gland involution (20), it enhances proliferation and prevents apoptosis in a variety of tumorigenic cells (13, 34). In our model of ErbB2-induced tumorigenesis, the Stat3$^{flx/flx}$/NIC tumors exhibited a 2-fold reduction in the number of proliferating cells but showed no change in apoptotic index compared with wild-type NIC tumors. The fact that the Stat3$^{flx/flx}$/NIC tumors did not exhibit increased apoptosis may reflect the fact that Stat3 ablation occurs before ErbB2-driven tumor induction, thus allowing for the selection of cells expressing Stat3-independent survival pathways. These observations suggest that tumor cells can be selected to survive in the absence of Stat3 but that activated ErbB2 tumors are at a proliferative disadvantage when lacking activated Stat3 expression.

Although several studies attempt to correlate the presence of activated Stat3 in human breast tumors with prognostic factors such as tumor stage, tumor size, or patient survival, few reports correlate Stat3 expression with breast cancer metastasis (1). Therefore, one of the most striking aspects of this study is the observation that Stat3-deficient tumors exhibit a dramatic impairment in their capacity to metastasize to the lung. Whereas Stat3 can regulate the transcription of proinvasive matrix metalloproteinases (33, 35), neither MMP2 nor MMP9 protein levels changed in NIC tumors in the absence of Stat3 expression (data not shown). However, we did observe that Stat3$^{flx/flx}$/NIC tumor cells were impaired in their ability to colonize and grow in the lung. Surprisingly, our microarray data did not reveal the differential expression of any genes directly implicated in metastasis. The absence of these genes further supports the hypothesis that Stat3 is involved in promoting metastasis via the up-regulation of several genes to illicit a prometastatic response (e.g., through the up-regulation of angiogenic and inflammatory responses) rather than direct transcriptional regulation of any one specific gene involved in invasion or metastasis. Thus, the impaired metastasis seen in both the Stat3$^{flx/flx}$/NIC mice and the primary Stat3-null tumor cells may indicate a general requirement for Stat3 in tumor cell dissemination, establishment, and/or growth at a secondary site.

In this model, the metastatic defect was also correlated with impaired tumor angiogenesis. Solid tumors that are impaired in vascularization are often limited in their ability to efficiently metastasize (36). Stat3-deficient tumors exhibited reduced expression of VEGF, which is considered a major mediator of the angiogenic process (36). Consistent with these observations, Stat3 expression corresponds with VEGF protein levels in a variety of transformed cell lines (37, 38). Additionally, down-regulating Stat3 activity by siRNA or through expression of a dominant-negative form causes a decrease in VEGF downstream of interleukin-6 in cervical cancer cells and Src and ErbB2 in human melanoma and breast cancer cells (39). More recently, expression of the activated mutant of Stat3, Stat3-Y705F, was positively correlated with microvessel density in human hepatocellular carcinoma tissue sections (14). Thus, the presence of Stat3 serves to promote the expression of VEGF and allow for tumor angiogenesis.

Published OnlineFirst August 18, 2009; DOI: 10.1158/0008-5472.CAN-09-1684

Although the above studies suggest that tumor cells are the principle source of VEGF, it has recently been reported that infiltrating tumor-associated macrophages can also contribute to VEGF production (40). It is thus interesting to note that gene expression profiling revealed a profound reduction in the expression of genes involved in both inflammatory and angiogenic responses in the Stat3-deficient tumors. Given that Stat3, also known as the APR factor, is a master regulator of this inflammation-based response (41), it is conceivable that impairment of inflammation through the down-regulation of this network may compromise the metastatic capacity of these tumors. In the normal mammary gland, activation of Stat3 and C/EBPδ during involution leads to an inflammatory cascade that is characterized by the recruitment and activation of leukocytes, partly via the expression of serum amyloid genes (19, 42), and by the production of various growth factors (20, 31, 43, 44).

In tumors, the recruitment of inflammatory cells, such as macrophages, and release of growth factors, such as VEGF, can potentiate angiogenesis and metastasis (31, 40, 45). Indeed, the recruitment of macrophages was shown to be critical in promoting metastatic progression in the PyVmT mammary tumor transgenic model (40). Recently, mammary-specific ablation of steroid receptor coactivator-1 in the PyVmT tumor model also resulted in a block in tumor metastasis (46). Significantly, the steroid receptor coactivator-1/Stat3 complex is involved in the transcriptional up-regulation of *cebpd* (ref. 47; Fig. 5*C*). The direct transcriptional targets of C/EBPδ include *saa1* and *saa2*, both of which are involved in the mobilization of immune cells during normal mammary gland involution and may serve a similar role in the tumor microenvironment, effectively engaging prometastatic immune cells such as macrophages (42). Thus, this transcription regulatory network is strongly implicated as a critical modulator of the metastatic process via the dysregulation of the APR, inflammation, and angiogenesis. The future development of therapeutics directed at suppressing this Stat3-dependent inflammatory cascade may be a promising treatment regime for metastatic breast cancers.

Disclosure of Potential Conflicts of Interest

No potential conflicts of interest were disclosed.

Acknowledgments

Received 5/8/09; revised 6/18/09; accepted 6/23/09; published OnlineFirst 8/25/09.

Grant support: National Cancer Institute of Canada/Terry Fox Foundation New Frontiers Program Project Team grant 017003, Canadian Institutes of Health Research Canada Graduate Scholarships Doctoral Award (J.J. Ranger), and McGill University Canadian Research Chair in Molecular Oncology (W.J. Muller).

The costs of publication of this article were defrayed in part by the payment of page charges. This article must therefore be hereby marked *advertisement* in accordance with 18 U.S.C. Section 1734 solely to indicate this fact.

We thank H. Lahlou and G. Ursini-Siegel for advice and discussions, T. Rao, R. Annan, and D. Dankort for critical reading of the article, and B. Schade for help with microarray experiments.

References

1. Hsieh FC, Cheng G, Lin J. Evaluation of potential Stat3-regulated genes in human breast cancer. Biochem Biophys Res Commun 2005;335:292–9.
2. Yeh YT, Ou-Yang F, Chen IF, et al. STAT3 Ser^{727} phosphorylation and its association with negative estrogen receptor status in breast infiltrating ductal carcinoma. Int J Cancer 2006;118:2943–7.
3. Yu H, Jove R. The STATs of cancer—new molecular targets come of age. Nat Rev Cancer 2004;4:97–105.
4. Ren Z, Schaefer TS. ErbB-2 activates Stat3α in a Src- and JAK2-dependent manner. J Biol Chem 2002;277:38486–93.
5. Garcia R, Yu CL, Hudnall A, et al. Constitutive activation of Stat3 in fibroblasts transformed by diverse oncoproteins and in breast carcinoma cells. Cell Growth Differ 1997;8:1267–76.
6. Bromberg JF, Horvath CM, Besser D, Lathem WW, Darnell JE, Jr. Stat3 activation is required for cellular transformation by v-src. Mol Cell Biol 1998;18:2553–8.
7. Bromberg JF, Wrzeszczynska MH, Devgan G, et al. Stat3 as an oncogene. Cell 1999;98:295–303.
8. Grandis JR, Drenning SD, Zeng Q, et al. Constitutive activation of Stat3 signaling abrogates apoptosis in squamous cell carcinogenesis *in vivo*. Proc Natl Acad Sci U S A 2000;97:4227–32.
9. Sumita N, Bito T, Nakajima K, Nishigori C. Stat3 activation is required for cell proliferation and tumorigenesis but not for cell viability in cutaneous squamous cell carcinoma cell lines. Exp Dermatol 2006;15:291–9.
10. Turkson J, Ryan D, Kim JS, et al. Phosphotyrosyl peptides block Stat3-mediated DNA binding activity, gene regulation, and cell transformation. J Biol Chem 2001;276:45443–55.
11. Zhang YW, Wang LM, Jove R, Vande Woude GF. Requirement of Stat3 signaling for HGF/SF-Met mediated tumorigenesis. Oncogene 2002;21:217–26.
12. Burke WM, Jin X, Lin HJ, et al. Inhibition of constitutively active Stat3 suppresses growth of human ovarian and breast cancer cells. Oncogene 2001;20:7925–34.
13. Al Zaid Siddiquee K, Turkson J. STAT3 as a target for inducing apoptosis in solid and hematological tumors. Cell Res 2008;18:254–67.
14. Yang SF, Wang SN, Wu CF, et al. Altered p-STAT3 (Tyr^{705}) expression is associated with histological grading and intratumour microvessel density in hepatocellular carcinoma. J Clin Pathol 2007;60:642–8.
15. Ma XT, Wang S, Ye YJ, Du RY, Cui ZR, Somsouk M. Constitutive activation of Stat3 signaling pathway in human colorectal carcinoma. World J Gastroenterol 2004;10:1569–73.
16. Abdulghani J, Gu L, Dagvadorj A, et al. Stat3 promotes metastatic progression of prostate cancer. Am J Pathol 2008;172:1717–28.
17. Raz R, Lee CK, Cannizzaro LA, d'Eustachio P, Levy DE. Essential role of STAT3 for embryonic stem cell pluripotency. Proc Natl Acad Sci U S A 1999;96:2846–51.
18. Ursini-Siegel J, Hardy WR, Zuo D, et al. ShcA signalling is essential for tumour progression in mouse models of human breast cancer. EMBO J 2008;27:910–20.
19. Suffredini AF, Fantuzzi G, Badolato R, Oppenheim JJ, O'Grady NP. New insights into the biology of the acute phase response. J Clin Immunol 1999;19:203–14.
20. Humphreys RC, Bierie B, Zhao L, Raz R, Levy D, Hennighausen L. Deletion of Stat3 blocks mammary gland involution and extends functional competence of the secretory epithelium in the absence of lactogenic stimuli. Endocrinology 2002;143:3641–50.
21. Finak G, Godin N, Hallett M, et al. BIAS: Bioinformatics Integrated Application Software. Bioinformatics (Oxford, England) 2005;21:1745–6.
22. Irizarry RA, Hobbs B, Collin F, et al. Exploration, normalization, and summaries of high density oligonucleotide array probe level data. Biostatistics (Oxford, England) 2003;4:249–64.
23. Smyth GK, Speed T. Normalization of cDNA microarray data. Methods (San Diego, CA) 2003;31:265–73.
24. Yang YH, Buckley MJ, Speed TP. Analysis of cDNA microarray images. Brief Bioinform 2001;2:341–9.
25. Hong F, Breitling R, McEntee CW, Wittner BS, Nemhauser JL, Chory J. RankProd: a bioconductor package for detecting differentially expressed genes in meta-analysis. Bioinformatics (Oxford, England) 2006;22:2825–7.
26. White DE, Kurpios NA, Zuo D, et al. Targeted disruption of β_1-integrin in a transgenic mouse model of human breast cancer reveals an essential role in mammary tumor induction. Cancer Cell 2004;6:159–70.
27. Kijima T, Niwa H, Steinman RA, et al. STAT3 activation abrogates growth factor dependence and contributes to head and neck squamous cell carcinoma tumor growth *in vivo*. Cell Growth Differ 2002;13:355–62.
28. Cantwell CA, Sterneck E, Johnson PF. Interleukin-6-specific activation of the C/EBPδ gene in hepatocytes is mediated by Stat3 and Sp1. Mol Cell Biol 1998;18:2108–17.
29. Clarkson RW, Boland MP, Kritikou EA, et al. The genes induced by signal transducer and activators of transcription (STAT)3 and STAT5 in mammary epithelial cells define the roles of these STATs in mammary development. Mol Endocrinol (Baltimore, MD) 2006;20:675–85.
30. Ray A, Ray BK. Serum amyloid A gene expression under acute-phase conditions involves participation of inducible C/EBP-β and C/EBP-δ and their activation by phosphorylation. Mol Cell Biol 1994;14:4324–32.
31. Stein T, Morris JS, Davies CR, et al. Involution of the mouse mammary gland is associated with an immune cascade and an acute-phase response, involving LBP, CD14 and STAT3. Breast Cancer Res 2004;6:R75–91.
32. Diaz N, Minton S, Cox C, et al. Activation of stat3 in primary tumors from high-risk breast cancer patients is associated with elevated levels of activated SRC and survivin expression. Clin Cancer Res 2006;12:20–8.
33. Xie TX, Wei D, Liu M, et al. Stat3 activation regulates the expression of matrix metalloproteinase-2 and tumor invasion and metastasis. Oncogene 2004;23:3550–60.
34. Frank DA. STAT3 as a central mediator of neoplastic cellular transformation. Cancer Lett 2007;251:199–210.
35. Dechow TN, Pedranzini L, Leitch A, et al. Requirement of matrix metalloproteinase-9 for the transformation of

Published OnlineFirst August 18, 2009; DOI: 10.1158/0008-5472.CAN-09-1684

human mammary epithelial cells by Stat3-C. Proc Natl Acad Sci U S A 2004;101:10602–7.
36. Carmeliet P. VEGF as a key mediator of angiogenesis in cancer. Oncology 2005;69 Suppl 3:4–10.
37. Niu G, Wright KL, Huang M, et al. Constitutive Stat3 activity up-regulates VEGF expression and tumor angiogenesis. Oncogene 2002;21:2000–8.
38. Xu Q, Briggs J, Park S, et al. Targeting Stat3 blocks both HIF-1 and VEGF expression induced by multiple oncogenic growth signaling pathways. Oncogene 2005; 24:5552–60.
39. Wei LH, Kuo ML, Chen CA, et al. Interleukin-6 promotes cervical tumor growth by VEGF-dependent angiogenesis via a STAT3 pathway. Oncogene 2003;22: 1517–27.
40. Lin EY, Li JF, Gnatovskiy L, et al. Macrophages regulate the angiogenic switch in a mouse model of breast cancer. Cancer Res 2006;66:11238–46.
41. Alonzi T, Maritano D, Gorgoni B, Rizzuto G, Libert C, Poli V. Essential role of STAT3 in the control of the acute-phase response as revealed by inducible gene inactivation [correction of activation] in the liver. Mol Cell Biol 2001;21:1621–32.
42. Pensa S, Watson C, Poli V. Stat3 and the inflammation/acute phase response in involution and breast cancer. J Mammary Gland Biol Neoplasia 2009;14:121–9.
43. Thangaraju M, Rudelius M, Bierie B, et al. C/EBPδ is a crucial regulator of pro-apoptotic gene expression during mammary gland involution. Development (Cambridge, England) 2005;132:4675–85.
44. Watson CJ. Immune cell regulators in mouse mammary development and involution. J Animal Sci 2008;87:35–42.
45. McDaniel SM, Rumer KK, Biroc SL, et al. Remodeling of the mammary microenvironment after lactation promotes breast tumor cell metastasis. Am J Pathol 2006;168:608–20.
46. Wang S, Yuan Y, Liao L, et al. Disruption of the SRC-1 gene in mice suppresses breast cancer metastasis without affecting primary tumor formation. Proc Natl Acad Sci U S A 2009;106:151–6.
47. Zhang Y, Sif S, DeWille J. The mouse C/EBPδ gene promoter is regulated by STAT3 and Sp1 transcriptional activators, chromatin remodeling and c-Myc repression. J Cell Biochem 2007;102:1256–70.

Cancer Research
The Journal of Cancer Research (1916–1930) | The American Journal of Cancer (1931–1940)

AACR American Association for Cancer Research

Identification of a Stat3-Dependent Transcription Regulatory Network Involved in Metastatic Progression

Jill J. Ranger, David E. Levy, Solmaz Shahalizadeh, et al.

Cancer Res 2009;69:6823-6830. Published OnlineFirst August 18, 2009.